Quasi-Harmonic Method For Studying Very Low Frequency Modes In Proteins

R. M. LEVY, A. R. SRINIVASAN, and W. K. OLSON, *Department of Chemistry, Rutgers, The State University of New Jersey, New Brunswick, New Jersey 08903;* and J. A. McCAMMON, *Department of Chemistry, University of Houston, Houston, Texas 77004*

Synopsis

A quasi-harmonic approximation is described for studying very low frequency vibrations and flexible paths in proteins. The force constants of the empirical potential function are quadratic approximations to the potentials of mean force; they are evaluated from a molecular dynamics simulation of a protein based on a detailed anharmonic potential. The method is used to identify very low frequency ($\sim$1 cm^{-1}) normal modes for the protein pancreatic trypsin inhibitor. A simplified model for the protein is used, for which each residue is represented by a single interaction center. The quasi-harmonic force constants of the virtual internal coordinates are evaluated and the normal-mode frequencies and eigenvectors are obtained. Conformations corresponding to distortions along selected low-frequency modes are analyzed.

INTRODUCTION

Collective motions of large numbers of atoms in a protein are known to have functional significance.[1-3] Thus, the identification of low-energy deformations and low-frequency modes of motion in proteins is an important goal of theoretical studies of the molecular-mechanics type. The traditional theoretical approach to the analysis of collective motions in ordered polymers has been to perform a harmonic analysis to obtain normal-mode frequencies and eigenvectors.[4-8] This approach is appealing for studying flexibility, because the low-frequency eigenvectors can be used directly to determine the paths along which the macromolecules are most readily deformed.[9] The force constants contained in the required second-derivative matrix are usually parameterized to fit the potential at a conformational minimum where the normal-mode expansion is exact. The parameterization is particularly useful for spectral identification and assignment of relatively high frequency modes. For the study of very low frequency modes, however, a force field should incorporate the anharmonic character with which the protein moves, since the effect of the anharmonicity can be to enhance significantly the flexibility.[10]

In this article, we introduce a "quasi-harmonic" approximation for studying collective motions and flexible paths in proteins. The model system studied is the pancreatic trypsin inhibitor (PTI). The atomic fluctuations obtained from a 96-ps molecular-dynamics simulation of PTI[11]

Biopolymers, Vol. 23, 1099–1112 (1984)

CCC 0006-3525/84/061099-14$04.00

are used to construct the "quasi-harmonic" force field and the normal-mode eigenvectors and frequencies of the protein are then evaluated. A principal assumption of the approximation is that the effective potential energy can be expressed as a quadratic function of the chosen coordinates. In contrast to the usual harmonic analysis, however, the effective force constants are obtained from a quadratic approximation to the potential of mean force, so that anharmonic effects are included implicitly.[12] The method and preliminary results are described below.

METHOD

In this section, we describe the quasi-harmonic oscillator approximation and introduce the specific form of the model used to study the very low frequency modes in PTI. In the quasi-harmonic approximation, temperature-dependent experimental or computer-simulation data are used to construct a quadratic model for the energy of the system as a function of atomic coordinates at each temperature. The quasi-harmonic approximation appears to have been first introduced by Kobayashi and Todokoro[13] to describe the temperature dependence of ir, Raman, and thermodynamic data for crystalline polyethylene. For the polyethylene analysis, experimental data concerning the temperature dependence of unit-cell dimensions were used, together with a harmonic model for the intermolecular forces to calculate the normal modes and frequencies of the orthorhombic polyethylene crystal between 10 and 300 K. Recently, quasi-harmonic oscillator models have been introduced to calculate optical spectra for small molecules from Monte Carlo simulations of molecular motion on anharmonic surfaces[14,15] and to evaluate the entropy of macromolecules using molecular-dynamics simulations.[16,17] Here, we describe how the quasi-harmonic oscillator approximation can be used to model large-scale aspects of protein motions.

The model used to describe PTI is based on the virtual-bond formulation introduced by Brant and Flory,[18] and subsequently used to describe polynucleotides,[19,20] polypeptides,[21,22] and proteins.[23–25] Each of the 58 amino acids is represented by a single interaction center; for the analysis below, each interaction center has been taken to coincide with the C^{α} position of the corresponding amino acid in the PTI crystal structure. These centers are linked by virtual bonds, virtual bond angles, and virtual dihedral angles. The use of a virtual-bond model greatly simplifies the computational task of finding the harmonic or quasi-harmonic normal modes and frequencies for the protein. For the full atomic model of PTI including all non-hydrogen atoms, finding the normal modes requires diagonalizing a 1500×1500 matrix, whereas only a matrix of order $(58 \times 3) = 174$ must be diagonalized for the virtual-bond model we use. The virtual-bond model is particularly appropriate for the study of the lowest frequency modes of proteins, which involve the collective motions of entire residues.

In the quasi-harmonic approximation, it is assumed that the empirical

potential-energy function can be expressed as a harmonic function of the internal coordinates. The most general expression for the quadratic potential is

$$E = \frac{1}{2}\sum_{ij} K_{ij}(q^i - q_0^i)(q^j - q_0^j) \tag{1}$$

where $(q^i - q_0^i)$ is the displacement of the ith internal coordinate from its equilibrium value, the K_{ii} are the diagonal force constants for bond stretching and angle and torsion bending, and the off-diagonal force constants K_{ij} arise from the possible coupling among the different internal coordinates. For this preliminary study of PTI using the virtual-bond model, we have assumed the off-diagonal force constants of Eq. (1) are much smaller than the diagonal force constants, and we have retained only the diagonal terms in the model. The empirical potential-energy function for the virtual-bond model is then expressed as

$$E(\mathbf{R}) = \frac{1}{2}\sum_{\substack{\text{virtual}\\ \text{bonds}}} K_b^i(b^i - b_0^i)^2 + \frac{1}{2}\sum_{\substack{\text{virtual}\\ \text{bond angles}}} K_\theta^i(\theta^i - \theta_0^i)^2 + \frac{1}{2}\sum_{\substack{\text{virtual}\\ \text{dihedral angles}}} K_\phi^i(\phi^i - \phi_0^i)^2 \tag{2}$$

The energy as given by Eq. (2) is a function of the Cartesian coordinate set (**R**) specifying the position of all the interaction centers, but the calculation is carried out by evaluating the coordinates for virtual bonds $\{b^i\}$, virtual bond angles $\{\theta^i\}$, and virtual dihedral angles $\{\phi^i\}$ for a given geometry (**R**). The temperature-dependent effective force constants of Eq. (2) are obtained in the quasi-harmonic approximation by equating the second moments of the virtual internal coordinate distributions determined by the harmonic potential, Eq. (2), with those evaluated from the complete molecular dynamics simulation[11] of PTI based on a detailed anharmonic potential[14–16]:

$$K_b^i = \frac{k_B T}{\langle (b^i - b_0^i)^2 \rangle} \tag{3a}$$

$$K_\theta^i = \frac{k_B T}{\langle (\theta^i - \theta_0^i)^2 \rangle} \tag{3b}$$

$$K_\phi^i = \frac{k_B T}{\langle (\phi^i - \phi_0^i)^2 \rangle} \tag{3c}$$

k_B is Boltzmann's constant, T is the absolute temperature, and the quantities in brackets $\langle\ \rangle$ are second moments of the virtual internal coordinate fluctuations calculated from the time average of the detailed atomic trajectory, e.g.,

$$\langle (b^i - b_0^i)^2 \rangle = \frac{1}{n}\sum_{t=1}^{n} (b_t^i - b_0^i)^2 \tag{4}$$

TABLE I
Mean-Square Fluctuations[a] of Virtual Internal Coordinates and Quasiharmonic Force Constants

	Mean	Maximum	Minimum	SD
$\langle(\Delta b)^2\rangle$ (Å^2)	0.0037	0.0048	0.0029	0.0004
K_b (kcal/mol Å^2)	161	206	125	
$\langle(\Delta\theta)^2\rangle$ (rad^2)	0.010	0.026	0.0031	0.0047
K_θ (kcal/mol rad^2)	60	193	23	
$\langle(\Delta\phi)^2\rangle$ (rad^2)	0.035	0.13	0.0066	0.024
K_ϕ (kcal/mol rad^2)	17	91	5	

[a] Mean-square fluctuations calculated from 96-ps trajectory (Ref. 11).

where b_t^i is the magnitude of the ith virtual bond at time t and n is the number of time points sampled. The magnitudes of the virtual bonds were sampled from 600 coordinate sets evenly spaced over the 100-ps PTI trajectory. From the results of a detailed analysis of the collective motions of PTI based on time-correlation functions,[26] we conclude that the 100-ps trajectory is long enough to adequately sample the lowest frequency collective modes of the protein. The mean square fluctuations of the virtual internal coordinates calculated from the PTI trajectory and the force constants obtained using Eq. (2) are listed in Table I. It is of interest to compare the virtual bond stretching and bond angle bending force constants calculated from the harmonic approximation to the potential of mean force (Table I) with values previously suggested from similar simplified representations of proteins.[21,23,27] The average value of the virtual bond stretching force constant calculated in the quasi-harmonic approximation is about twice that used previously ($\overline{K}_b$ = 161 kcal/mol Å^2, Table I; 80 kcal/mol Å^2, Ref. 23), while the quasi-harmonic bond bending force constants are somewhat smaller ($\overline{K}_\theta$ = 60 kcal/mol rad^2, Table I; 80 kcal/mol rad^2, Ref. 23). The virtual torsion angle force field used in earlier studies of simplified polypeptide models were not harmonic, so that a direct comparison with the quasi-harmonic torsion force constants of Table I cannot be made.

The normal-mode frequencies obtained from the quasi-harmonic potential [Eq. (2)] are solutions of the secular equation

$$|\mathbf{F} - \omega^2\mathbf{T}| = 0 \tag{5}$$

Where $\mathbf{F}$ is the matrix of second derivatives of the potential energy ($F_{ij} = d^2E/dx_i\,dx_j$) and $\mathbf{T}$ is the diagonal kinetic energy matrix ($T_{ij} = \delta_{ij}m_i$); for this preliminary study, the masses of each of the 58 residues were set equal to the average value, 100 a.m.u. Of the $3N$ eigenvalues of Eq. (4), $3N$-6 correspond to normal-mode frequencies ω_i, with associated eigenvectors $\mathbf{Q}_i$; the components of $\mathbf{Q}_i$ give the relative amplitudes of the contributing atomic displacements expressed as mass scaled Cartesian coordinates. In order to examine structural features of the low-frequency vibrations, a set of structures corresponding to motion along normal coordinates can be

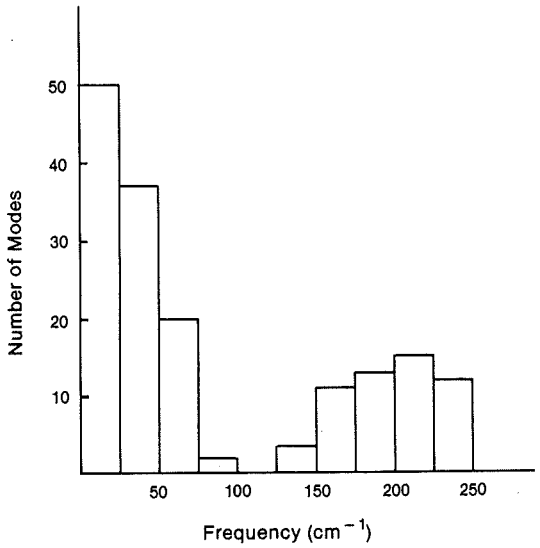

Fig. 1. Histogram of frequency distribution obtained from the normal-mode analysis of the simplified PTI model.

generated by adding normal coordinate displacement vectors to the minimum-energy coordinates:

$$\mathbf{X}_i = \mathbf{X}_{\min} + \frac{(k_B T)^{1/2}}{\omega^i} \mathbf{M}^{-1/2} \mathbf{Q}_i \tag{6}$$

here $\mathbf{X}_{\min}$ are the energy-minimized coordinates of the C^α atoms, $\mathbf{Q}_i$ is a mass-weighted normal coordinate eigenvector, $\mathbf{M}^{-1/2}$ is a diagonal matrix with elements $M^{-1/2}$ that cancels the mass dependence in the components of Q_i, and the scale factor $(k_B T)^{1/2}/\omega_i$ adjusts the displacements to the same total energy $k_B T$ in each mode.

RESULTS AND DISCUSSION

The frequency distribution for the simplified PTI model obtained in the quasi-harmonic approximation is shown in Fig. 1. This simplified PTI model has 168 nonzero vibrational frequencies. The highest frequency modes at ~250 cm^{-1} correspond to localized stretches of virtual bonds. For comparison, the average stretching frequency for an isolated pair of adjacent residues is calculated to be 210 cm^{-1} using the mean value $\overline{K}_b$ = 161 kcal/mol Å^2 (Table I). The lowest frequency mode calculated from the model is 0.32 cm^{-1}. This value is considerably smaller than a previous estimate (~30 cm^{-1}, Ref. 28) of the lowest frequency of vibration for globular proteins based on a uniform continuous elastic model, although it is close to the value (~0.17 cm^{-1}, Ref. 23) obtained from a molecular-dynamics simulation of PTI based on a similar simplified representation

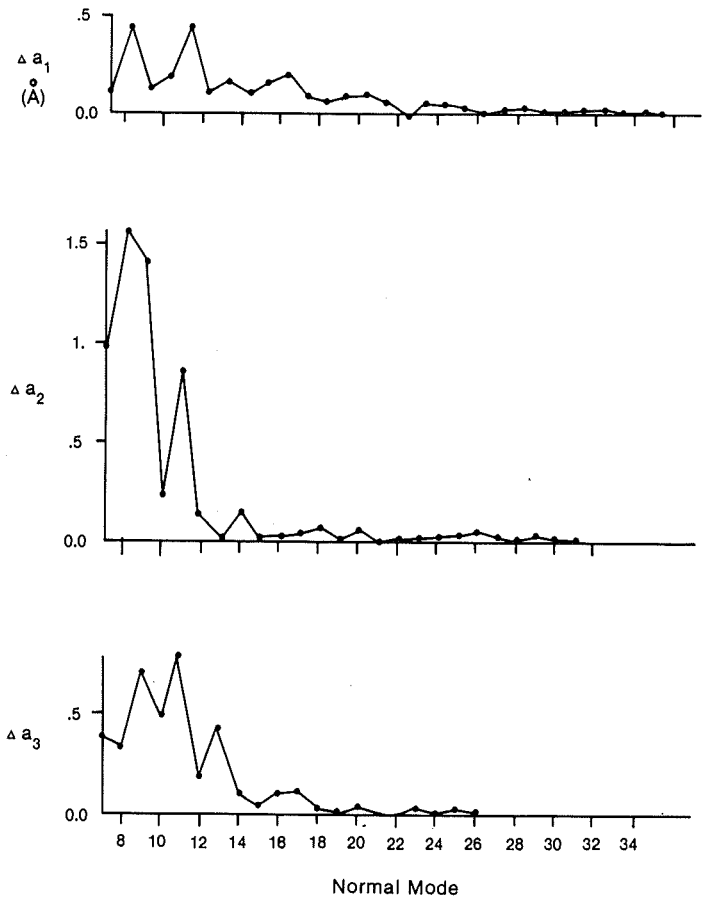

Fig. 2. Changes in the principal values of the root-mean-square second moments of atomic positions for displacements with k_BT strain energy at 300 K along the lowest frequency modes.

of the protein. Theoretical studies[26,29–31] of protein flexibility using detailed atomic models have demonstrated that the protein atoms move in highly anisotropic, inhomogeneous environments. As discussed below, the lowest vibrational frequencies correspond to the collective motions of structural units of the protein, which are constrained by relatively weak van der Waals interactions. Indeed, collective vibrations with frequencies $\omega = 3$ cm^{-1} have been observed in detailed molecular-dynamics simulations of PTI,[26] and even lower frequency vibrations were predicted. With the quasi-harmonic force field and our simplified PTI molecular model, we find 50 vibrational modes with frequencies less than 25 cm^{-1} and 7 with frequencies less than 1 cm^{-1}.

The second moments of the distribution of atomic positions of a molecule a_i^2 (i = 1,2,3) provide a general measure of molecular shape.[32,33] For the

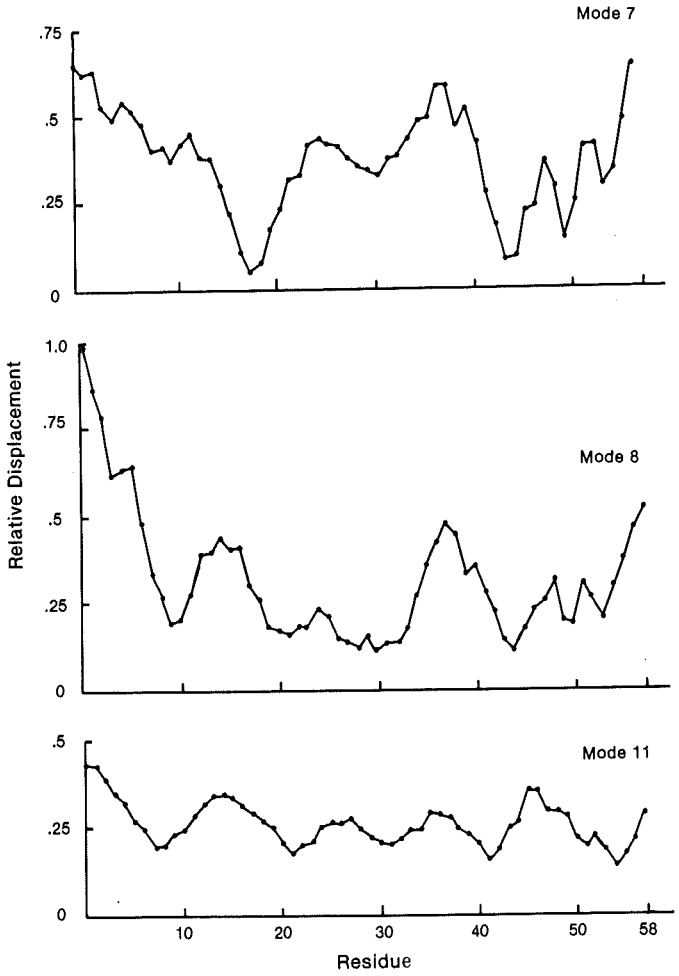

Fig. 3. Relative displacements of each of the residues along modes 7, 8, and 11. The displacements are normalized to the largest eigenvector component for these three modes, ($|\Delta \mathbf{r}|$ of residue 1 in mode 8).

simplified model of PTI we consider, they are related to the three moments of inertia, λ_i, of the molecule by $a_i^2 = \lambda_i^2 M$. PTI is roughly pear-shaped, with rms second moments $a_1 = 8.68$ Å, $a_2 = 4.75$ Å, $a_3 = 3.88$ Å. In order to identify low-frequency modes along which the entire PTI molecule is most easily deformed, we compare the square roots of the second moments, a_i, for molecular conformations corresponding to deformations along each of the normal-mode eigenvectors with the values for the x-ray structure. The changes in the a_i for displacements [Eq. (6)] along the lowest frequency modes are shown in Fig. 2. It is apparent that only for a very small number of the 168 modes (the lowest 10) do the vibrations change the overall shape

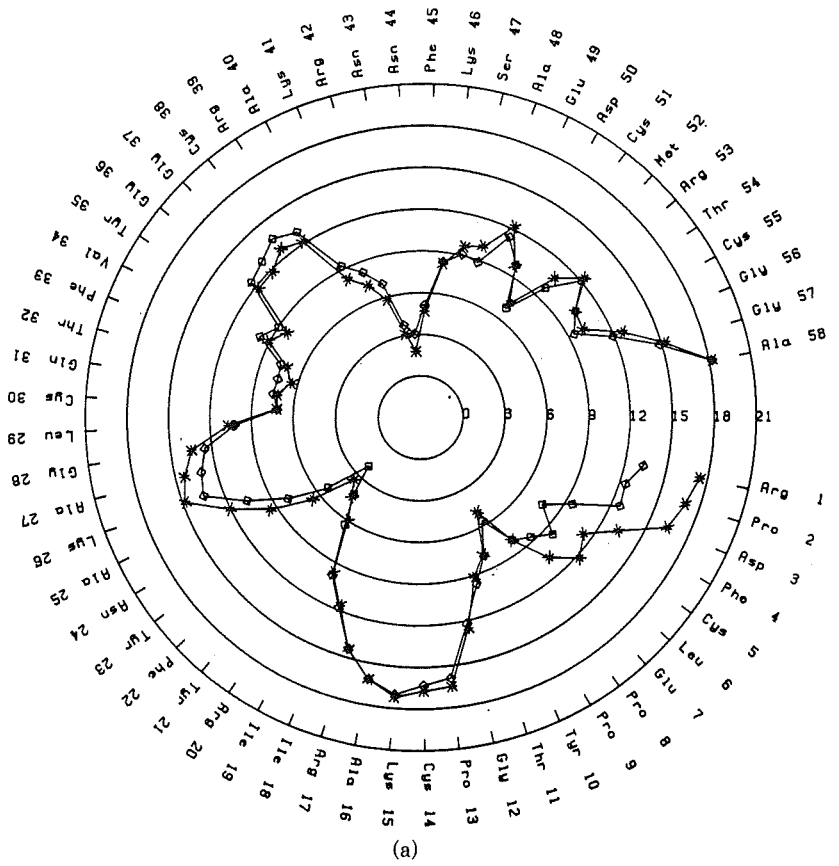

(a)

Fig. 4. Displacements from the center of mass (with k_BT strain energy) for each of the residues for modes 8 and 11. The circular "conformation wheel" format has been used to draw the graph (Refs. 36,37). (a) □, crystal structure (Ref. 48); *, mode 8; (b) □, crystal structure; *, mode 11.

of the molecule. The greatest distortion of the long axis of PTI occurs for displacements along mode 11, for which there is a 5% change in a_1 calculated with k_BT strain energy in this mode. Motion along mode 11 also results in the largest (20%) distortion of the a_3 axis. With regard to the remaining principal axis, a_2, the largest change is calculated to occur for displacements along mode 8. The large fractional change in a_2 (30%) is due to the motion of the N-terminal α-helix along the a_2 axis. It is of interest that the lowest frequency vibration (mode 7, 0.32 cm^{-1}) does not lead to the largest change in the dimensions of the molecule. We have obtained additional structural information concerning conformations obtained from motion [Eq. (6)] along modes 7, 8, and 11. The results are described below.

PTI contains two stretches of α-helix at the N- and C-termini (residues 3–6 and 47–56) and an antiparallel β-sheet oriented along the long axis of

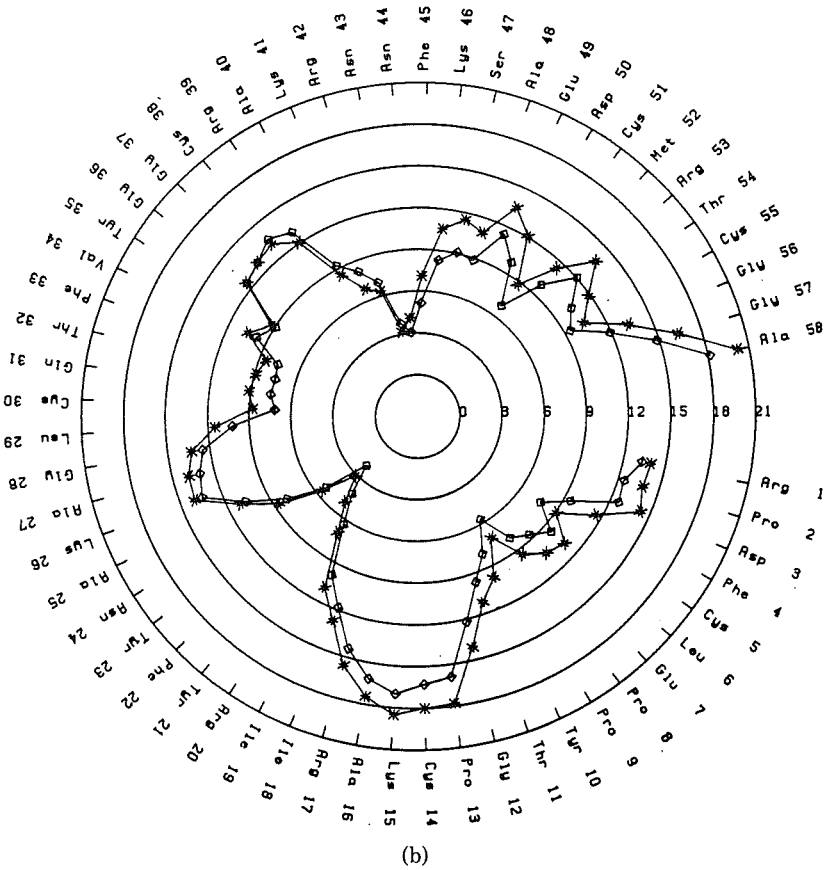

(b)

Fig. 4. (*continued from the previous page*)

the molecule (residues 16–25 and 28–35). There are three loop regions where the α-carbon chain direction is reversed: residues 14–16 (at the active site) and 37–39 at the top of the "pear" and residues 26–28 at the base. The relative displacements of each of the 58 C^{α} carbons along modes 7, 8, and 11 are shown in Fig. 3. The greatest displacements occur at the chain ends and in the loop regions. The pattern of the displacements in Fig. 3 can be most clearly interpreted in terms of collective motions of structural domains for mode 8. While the greatest displacements are at the N-terminal end, both loops at the top of the molecule appear to be moving collectively. The large displacements at residues 15 and 38 and the small displacements (approximate nodes) at residues 10, 21 and 31, 45 suggest that in mode 8, the two loops are bending and/or twisting with respect to the base of the molecule. In the full molecular-dynamics simulation of PTI[11,29] from which the quasi-harmonic force constants were derived, the largest displacements were observed to occur at the ends and in the loop regions of the protein. That similar trends for the displacements

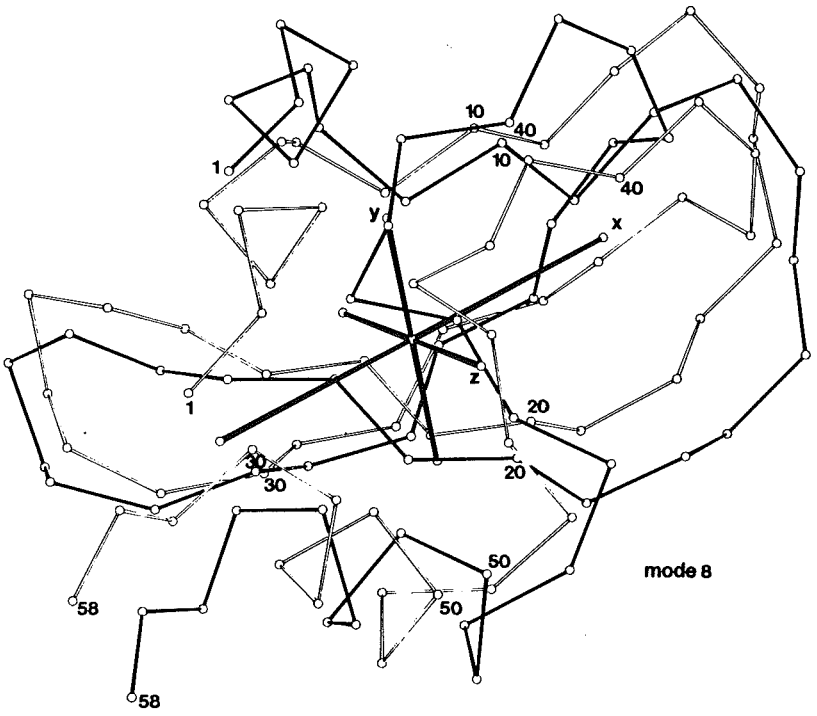

(a)

Fig. 5. ORTEP plots of the α-carbon skeleton of PTI displaced along modes 8 (a) and 11 (b): O═O, crystal structure; O—O, displaced structure along specified mode.

are found for the lowest frequency modes in the present study supports the suggestion[10,26,31,34,35] that low-frequency collective modes play the dominant role in determining atomic displacements.

The one-dimensional radial distributions of atomic displacements from the molecular center of mass along modes 8 and 11 are displayed as conformation wheels[33,36,37] in Fig. 4. Comparing the radial distributions for the molecule distorted along mode 8 with that for the crystal structure [Fig. 4(a)], it is apparent the N-terminal α-helix, residues 1–6, is moving as a unit away from the molecular center of mass, leading to the large change in a_2 calculated for this mode. Mode 11 has been identified as leading to the largest changes in dimension along the a_1 and a_3 principal axes. From the circular plot of radial distribution [Fig. 4(b)], it appears this mode resembles a very low frequency elastic-breathing vibration in that most of the atomic centers (53 out of 58) are increasing their radial distance from the center of mass in a coherent manner as the molecule is distorted along the normal coordinate. We present ORTEP plots of the α-carbon skeleton distorted along modes 8 and 11 in Fig. 5. For comparison, plots of the x-ray structure are included. The motions of the N- and C-terminal α-helices and of the loops at the top and at the base can be clearly seen in the pictures.

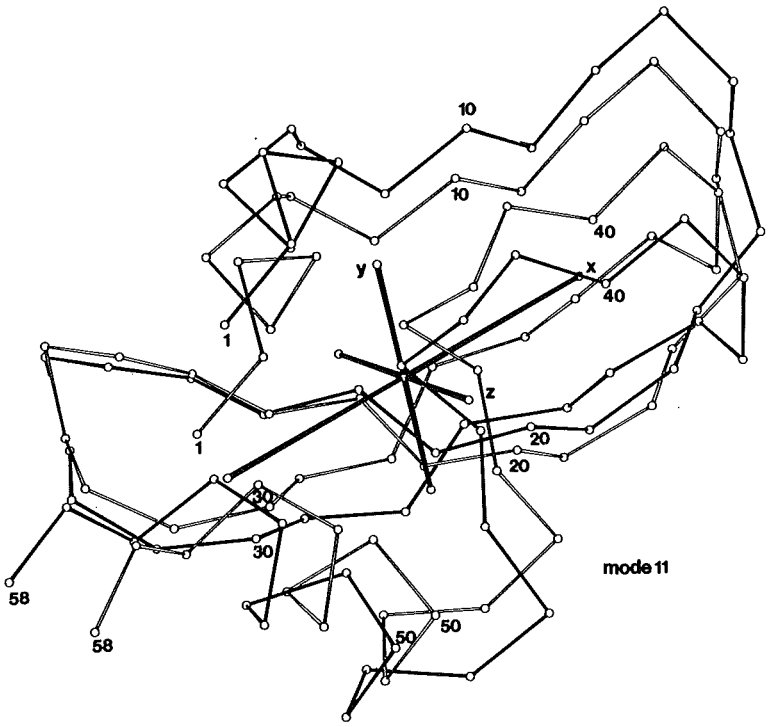

(b)

Fig. 5. (*continued from the previous page*)

The modeling of crystalline materials in terms of normal modes has long provided a framework for analyzing the thermodynamic characteristics of these systems. Although for globular proteins the normal-mode picture constitutes an approximate description of the complicated dynamics, the model is nevertheless finding increasing applications in analysis of experimental data for proteins. Of particular interest is the interpretation of calorimetric data for ligand binding in terms of changes in the vibrational density of states for the protein on ligand binding.[38] The vibrational density of states for a protein can be probed using optical techniques.[39–41] The recent availability of high-intensity synchrotron sources makes inelastic neutron scattering a very promising technique for probing the vibrational spectrum of protein. The low-frequency neutron scattering spectrum for lysozyme[42] and hexokinase[43] have been reported and experiments on PTI are underway. To aid in the interpretation of these experiments, theoretical vibrational normal- mode calculations of proteins are required. Three separate calculations of the vibrational spectrum and normal modes for PTI in the harmonic approximation have recently been reported.[34,35,44] For two of the calculations[34,35] the number of degrees of freedom considered is restricted to the dihedral angles of the protein, while for the third[44] the complete conformational space is considered; to solve the secular equation a 1500 × 1500 matrix diagonalization was required.[44]

In agreement with the quasi-harmonic analysis, the harmonic normal-mode results predict that the atomic functions were dominated by the low-frequency modes and that the loop regions and ends of PTI are the most flexible. The calculated density of states profiles in the harmonic approximation appear similar in that there is a peak in the density at ~30–50 cm^{-1} with the lowest frequency vibration calculated to occur at ~3 cm^{-1}. That the lowest frequencies calculated in the harmonic approximation are greater than the quasi-harmonic values may arise from the inclusion of anharmonic effects in the present calculation. However, the use of a simplified virtual-bond model for which we have not explicitly included nonbonded terms between residues may also lead to lower frequencies. The quasi-harmonic oscillator method we have developed to calculate the normal modes of PTI can be used with a more detailed atomic model for the protein, and such a calculation is underway for PTI (B. Brooks and M. Karplus, private communication).

In this paper, we have presented a new method for parameterizing a force field that can be used to study very low frequency vibrations and flexible paths in proteins. Since we are concerned here with the macromolecular features of the protein, a highly simplified model has been used for which entire residues are represented by single interaction centers. In the quasi-harmonic approximation, the effective force constants for these internal coordinates were obtained from a quadratic approximation to the potentials of mean force evaluated from a molecular-dynamics simulation of PTI on the full potential surface. The method is similar in spirit to the method proposed by Karplus and Kushick[45] for the evaluation of the entropy of macromolecules from molecular-dynamics simulations. A detailed comparison of the use of the harmonic approximation for the evaluation of the conformational entropy of a polypeptide with the quasi-harmonic approximation will be presented elsewhere.[16] The quasi-harmonic modeling of large-scale aspects of protein dynamics will be useful in a variety of applications. As illustrated here, quasi-harmonic models allow for a relatively simple and compact description of low-frequency, collective thermal motions in proteins. The effective energy function can be used for approximate determination of the large-scale responses of a protein to applied stresses prior to detailed calculations using the full energy function. Such calculations could be valuable in studies of the coupling of local and collective motions that occurs in ligand binding and other functional processes in proteins.[1–3,26,31,46,47] By associating solvent friction terms and corresponding random forces with the interaction centers, one would obtain a generalized version of a model that was used previously to analyze single group motions in the protein interior.[12,26,46] Such generalized models could be used to improve the level of description of solvent damping effects on large-scale motions of proteins.[2] The level of atomic detail incorporated in the model described here can be increased in several ways, including the introduction of hydrogen-bond–like interactions between residues to account more explicitly for protein secondary structures, the introduction

of terms to represent nonbonded interactions, and the use of more detailed models for the amino acid residues. It is important to identify the level of atomic detail that is required, since with increasing detail, it becomes difficult to interpret the results in terms of macromolecular motions.

This work has been supported by grants from the Petroleum Research Fund of the American Chemical Society (to R.M.L.) and the National Institutes of Health (to R.M.L., W.K.O., and J.A.M.). J.A.M. also acknowledges support from the NSF and the Robert A. Welch Foundation. R.M.L. and J.A.M. are recipients of National Institutes of Health Research Career Development Awards and Alfred P. Sloan Fellowships. J.A.M. is a Camille and Henry Dreyfus Teacher-Scholar.

References

1. Karplus, M. & McCammon, J. A. (1981) *CRC Crit. Rev. Biochem.* **9,** 293–357.
2. McCammon, J. A. & Northrup, S. H. (1981) *Nature* **293,** 316–317.
3. McCammon, J. A., Gelin, B. R., Karplus, M. & Wolynes, P. G. (1976) *Nature* **262,** 325–326.
4. Peticolas, W. (1978) *Methods Enzymol.* **61,** 425–458.
5. Gō, M. & Gō, N. (1976) *Biopolymers* **15,** 1119–1127.
6. Rabolt, J. F., Moore, W. H. & Krimm, S. (1977) *Macromolecules* **10,** 1065–1074.
7. Itoh, K. & Schimanouchi, T. (1970) *Biopolymers* **9,** 383–399.
8. Levy, R. M. & Karplus, M. (1979) *Biopolymers* **18,** 265–2495.
9. Sheridan, R. P., Levy, R. M. & Englander, S. W. (1984) *Proc. Natl. Acad. Sci. USA* **80,** 5569–5572.
10. Levy, R. M., Perahia, D. & Karplus, M. (1982) *Proc. Natl. Acad. Sci. USA* **79,** 1346–1350.
11. Karplus, M. & McCammon, J. A. (1979) *Nature* **277,** 578–580.
12. McCammon, J. A., Wolynes, P. G. & Karplus, M. (1979) *Biochemistry* **18,** 927–942.
13. Kobayashi, M. & Tadokoro, H. (1977) *J. Chem. Phys.* **66,** 1258–1265.
14. Levy, R. M., Rojas, O. & Friesner, R. (1984) *J. Phys. Chem.*, in press.
15. Friesner, R. & Levy, R. M. (1984) *J. Chem. Phys.*, in press.
16. Levy, R. M., Karplus, M., Kushick, J. & Perahia, D. (1984) *Macromolecules*, in press.
17. DiNola, A., Berendson, H. J. T. & Edholm, O. (1984) *Macromolecules*, in press.
18. Brant, D. A. & Flory, P. J. (1965) *J. Am. Chem. Soc.* **87,** 2791–2800.
19. Olson, W. & Flory, P. (1972) *Biopolymers* **11,** 1–23.
20. Srinivasan, A. R. (1976) *Curr. Sci.* **45,** 533–534.
21. McCammon, J. A., Northrup, S. H., Karplus, M. & Levy, R. M (1980) *Biopolymers* **19,** 2033–2045.
22. Srinivasan, A. R. & Rao, V. S. R. (1972) *J. Polym. Sci. A-2* **10,** 693–697.
23. Levitt, M. (1976) in *Models for Protein Dynamics, CECAM Workshop Report*, Universite de Paris XI, Orsay, France.
24. Srinivasan, R., Balasubramanian, R. & Rajan, S. S. (1976) *J. Mol. Biol.* **98,** 739–747.
25. Rackovsky, S. & Scheraga, H. A. (1978) *Macromolecules* **11,** 1168–1174.
26. Swaminathan, S., Ichiye, T., van Gunsteren, W. & Karplus, M. (1982) *Biochemistry* **21,** 5230–5241.
27. Levitt, M. (1976) *J. Mol. Biol.* **104,** 59–107.
28. Suzeuki, Y. & Go, N. (1975) *Int. J. Pept. Protein Res.* **7,** 333–334.
29. McCammon, J. A., Gelin, B. R., Karplus, M. & Wolynes, P. G. (1976) *Nature* **262,** 325–326.
30. Mao, B., Pear, M. R., McCammon, J. A. & Northrup, S. H. (1982) *Biopolymers* **21,** 1979–1990.

31. Morgan, J. D., McCammon, J. A. & Northrup, S. A. (1983) *Biopolymers* **22,** 1579–1594.
32. Flory, P. J. (1973) *Proc. Natl. Acad. Sci. USA* **70,** 1819–1823.
33. Olson, W. K. & Srinivasan, A. R. (1984) Preprint.
34. Go, N. (1983) *Proc. Natl. Acad. Sci. USA* **80,** 3696–3700.
35. Levitt, M., Sander, C. & Stern, P. (1984) *Int. J. Quantum Chem.*, in press.
36. Srinivasan, A. R. & Olson, W. K. (1980) *Int. J. Pept. Protein Res.* **16,** 111–123.
37. Srinivasan, A. R. & Yathindra, N. (1978) *Biopolymers* **17,** 1595–1600.
38. Sturtevant, J. (1977) *Proc. Natl. Acad. Sci. USA* **74,** 2236–2240.
39. Brown, K. G., Erforth, S. C., Small, E. W. & Peticolas, W. L. (1972) *Proc. Natl. Acad. Sci. USA* **69,** 1467–1469.
40. Peticolas, W. L. (1978) *Methods Enzymol.* **61,** 421–458.
41. Tasumi, M., Takeuchi, H., Ataka, S., Dwivedi, A. & Krimm, S. (1982) *Biopolymers* **21,** 711–714.
42. Bartunik, H., Jolles, P., Berthou, J. & Dianoux, A. (1982) *Biopolymers* **21,** 43–50.
43. Jacrot, B., Cusack, S., Dianoux, A. & Engleman, D. (1982) *Nature* **300,** 84–86.
44. Brooks, B. & Karplus, M. (1983) *Proc. Natl. Acad. Sci. USA* **80,** 6571–6575.
45. Karplus, M. & Kushick, J. (1981) *Macromolecules* **14,** 325–332.
46. Berkowitz, M. & McCammon, J. A. (1981) *J. Chem. Phys.* **75,** 957–961.
47. McCammon, J. A., Lee, C. Y. & Northrup, S. H. (1983) *J. Am. Chem. Soc.* **105,** 2232–2237.
48. Deisenhofer, J. & Steigeman, N. (1975) *Acta Crystallogr., Sect. B* **31,** 238–250.

Received May 31, 1983
Accepted November 11, 1983